7.2 MEASUREMENTS OF THE VON KÁRMÁN CONSTANT IN THE ATMOSPHERIC SURFACE LAYER—FURTHER DISCUSSION

Edgar L Andreas[1*], Kerry J. Claffey[1], Christopher W. Fairall[2], Andrey A. Grachev[2,3], Peter S. Guest[4], Rachel E. Jordan[1], and P. Ola G. Persson[2,3]

[1]U.S. Army Cold Regions Research and Engineering Laboratory, Hanover, New Hampshire
[2]NOAA Environmental Technology Laboratory, Boulder, Colorado
[3]Cooperative Institute for Research in Environmental Sciences, University of Colorado, Boulder, Colorado
[4]Naval Postgraduate School, Monterey, California

1. WAGENINGEN, 2002

At the last symposium in this series, in Wageningen, The Netherlands, we reported on new measurements of the von Kármán constant, k, in the atmospheric surface layer (Andreas et al. 2002). Figure 1 summarizes our understanding of these measurements at that time. At low values of the roughness Reynolds number, $Re_* = u_* z_0 / \nu$—where u_* is the friction velocity, z_0 is the roughness length, and ν is the kinematic viscosity of air—our data tended to support the constant value k = 0.421 that McKeon et al. (2004) measured in aerodynamically smooth flow in the Princeton Superpipe. At larger roughness Reynolds numbers, in aerodynamically rough flow, k decreased distinctly with Re_*. We were able to represent k in both regimes with a single analytical function of Re_*.

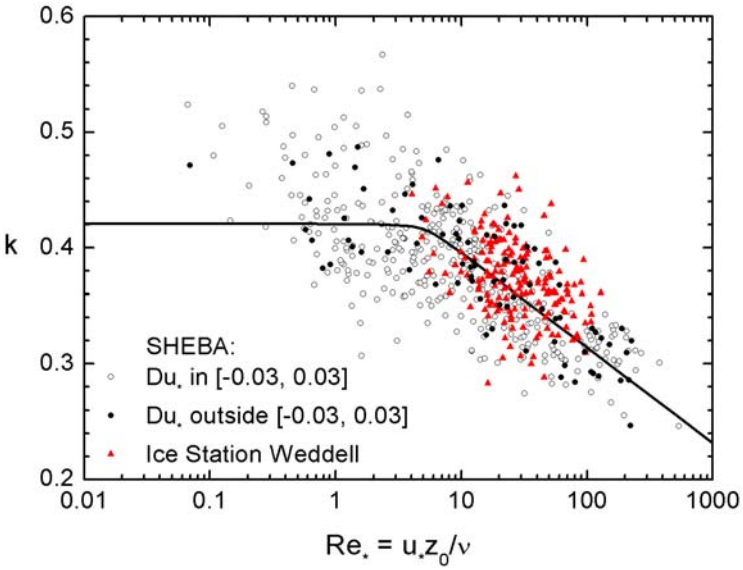

Fig. 1. Values of the von Kármán constant k obtained during the SHEBA experiment and on Ice Station Weddell that we reported at the last symposium in this series (Andreas et al. 2002). Du_* quantifies the vertical divergence in the SHEBA u_* profiles and is calculated from (5). There are 178 ISW and 453 SHEBA values shown; of the SHEBA values, 83 have Du_* in $[-0.03, 0.03]$. The line is an analytical fit to the data.

We have since realized, however, that we had not properly accounted for stratification effects on the k values depicted in Fig. 1. When we account for these stratification effects, the corrected k values do not have quite the range exhibited in Fig. 1. Furthermore, the dependence of these revised k values on roughness Reynolds number is statistically indistinguishable from the artificial correlation between k and Re_* that results from their shared variables. To get around this artificial correlation, we estimated Re_* with a bulk flux calculation and found k to have no correlation with this bulk estimate of Re_*. In other words, our measured k values exhibit large scatter that cannot be explained as a dependence on the roughness Reynolds number. Let us elaborate.

2. MEASUREMENTS AND ANALYSES

We based our evaluations of k on two large data sets collected over polar sea ice. One set came from the Arctic, from SHEBA, the yearlong experiment to study the Surface Heat Budget of the Arctic Ocean (Andreas et al. 1999; Persson et al. 2002; Uttal et al. 2002). Andreas et al. (2002)

*Corresponding author address: Edgar L Andreas, U.S. Army Cold Regions Research and Engineering Laboratory, 72 Lyme Road, Hanover, New Hampshire 03755-1290; e-mail: eandreas@crrel.usace.army.mil.

describe how we obtained the von Kármán constant from this set.

Our second set came from the Antarctic, from Ice Station Weddell (ISW). Andreas and Claffey (1995) describe our measurements of the wind speed profile on ISW, and Andreas et al. (2004a) explain the turbulence measurements that yield u_*.

For completeness, we briefly describe our analyses. During both SHEBA and Ice Station Weddell, we measured the hourly averaged profile of mean wind speed U(z) at height z in the atmospheric surface layer. Monin-Obukhov similarity theory predicts the following functional form for this profile:

$$U(z) = \frac{u_*}{k}\left[\ln(z/z_0) - \psi_m(z/L)\right] . \qquad (1)$$

Here, L is the Obukhov length, which we measured by eddy-correlation at both SHEBA and ISW, and ψ_m is a known function of the stratification parameter z/L.

Equation (1) actually derives from the more fundamental Monin-Obukhov similarity expression that relates the vertical wind speed gradient in the surface layer to u_*, z, k, and L;

$$\frac{\partial U}{\partial z} = \frac{u_*}{kz}\phi_m(z/L) , \qquad (2)$$

where ϕ_m is another known similarity function related to ψ_m (Panofsky 1963; Paulson 1970).

We carefully screened both the SHEBA and Ice Station Weddell data and analyzed only cases in which the flow was unobstructed, the sensors were well aligned with the wind, and all profile levels yielded usable data. We further required that the measured wind speed be at least $4\ m\ s^{-1}$ at each level to push the stratification toward neutral in these polar conditions, where the turbulent surface heat fluxes are rarely large. Lastly, we computed the correlation between U(z) and ln(z), as suggested by (1), with the ψ_m term neglected, and kept only cases for further analysis that had correlation coefficients of at least 0.99. That is, in all cases that we analyzed, U(z) was essentially linear in ln(z). Andreas and Claffey (1995) and Andreas et al. (2002) show sample profiles that survived our screening and explain that screening more fully.

Our correlation analysis of each profile yielded the slope

$$S = \frac{u_*}{k} \qquad (3)$$

and the intercept

$$I = -S\ln(z_0) \qquad (4)$$

for (1), still ignoring the ψ_m term. Since we measured the friction velocity, u_*, by eddy-correlation, we could evaluate k from (3); the roughness length, z_0, comes directly from (4).

On Ice Station Weddell, we had a single eddy-correlation measurement of u_*. But for all the SHEBA profiles used in this analysis, we had five independent measurements of u_* at heights between 2 and 18 m, nominally. Again, all values are based on hourly averages. We extrapolated this SHEBA u_* profile to the surface to get the actual surface value of the friction velocity, u_{*0}, which is a more fundamental quantity for analyses such as these (cf. Tennekes 1973). In all subsequent references to the friction velocity for the SHEBA data, we mean this surface value.

With five levels of u_* measurements from SHEBA, we could also evaluate the constant momentum flux assumption that underlies Monin-Obukhov similarity theory. Andreas et al. (2002) therefore introduce the u_* divergence parameter

$$Du_* = \frac{\partial u_*}{\partial \ln z}\frac{\langle \ln z \rangle}{u_{*0}} . \qquad (5)$$

Here, $\partial u_*/\partial \ln z$ is the least-square slope of the measured u_* profile as a function of ln(z), and $\langle \ln z \rangle$ is the average of the five ln(z) values.

Andreas et al. (2002) show a preliminary plot of k as a function of Du_* and define the Du_* region [–0.03, 0.03] as the constant flux regime. Eighty-three of the 453 SHEBA profiles that survived our screening are within this interval and are, presumably, our "best" data. Figure 1 divides the SHEBA data into cases that are within and outside this Du_* interval. Although sorting on Du_* eliminated the largest k values, the filled and open circles representing the SHEBA data in Fig. 1 do not otherwise seem to have different distributions. The Ice Station Weddell data in Fig. 1 are also compatible with the SHEBA set.

This latter observation is crucial and argues for the quality of our measurements. The SHEBA and Ice Station Weddell measurements were quite different. On ISW, we measured the wind speed

profile with propeller anemometers at four heights between 0.5 and 4 m. We measured the turbulent fluxes with an ATI (Applied Technologies, Inc.) sonic anemometer/thermometer mounted at a height of 4.65 m. At SHEBA, we measured the wind speed profile *and* the turbulent fluxes with five ATI sonics at heights between 2 and 18 m. In summary, we used different technologies and measurement heights for our profile measurements on ISW and at SHEBA, but the tendencies in the data sets seem indistinguishable.

3. STRATIFICATION CORRECTIONS

We felt that requiring high wind speed over sea ice would ensure that all the cases we analyzed for the von Kármán constant would feature near-neutral stratification. Further, Andreas and Claffey (1995) used a bulk Richardson number to verify that the stratification for the ISW profiles was near neutral. And Andreas et al. (2002) required that all SHEBA cases have $|10\,m/L_{med}|<0.1$, where 10 m is the nominal height of our SHEBA measurements and L_{med} is the median Obukhov length from our five SHEBA eddy-correlation measurements.

After our Wageningen presentation, however, we realized that the von Kármán constants that we presented still suffered from a residual stratification effect. Figure 2 shows the original SHEBA k values as a function of stratification, $<z>/L$, where $<z>$ is the geometric mean height of the five profile levels. Figure 3 shows a similar plot of the Ice Station Weddell values. Despite the fact that $|<z>/L|<0.1$ for all our measurements of k, these still exhibit an obvious stability dependence.

The lines in these two figures represent the stability-affected (uncorrected) von Kármán constants from (3) as

$$k_{uc} = \frac{k}{\phi_m(z/L)} \quad . \qquad (6)$$

Here, we use k = 0.40; and

$$\phi_m(z/L) = \left[1-16(z/L)\right]^{-1/4} \qquad (7a)$$

for z/L < 0 (Paulson 1970), and

$$\phi_m(z/L) = 1+5(z/L) \qquad (7b)$$

for z/L > 0 (Dyer 1974). Although (6) represents the trends in the k values well in Figs. 2 and 3, it does not necessarily pass through the centroids of the data clouds because k at neutral stratification is not 0.40 in our data sets.

Using (6) and (7), we can correct our original SHEBA and ISW k values for these residual stratification effects;

$$k_{sc} = k_{uc}\,\phi_m(z/L) \quad . \qquad (8)$$

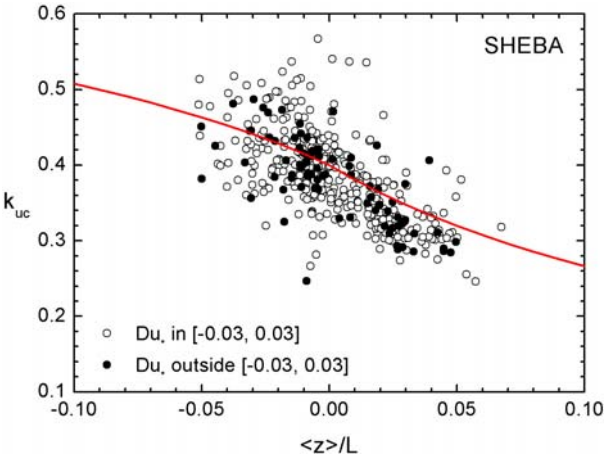

Fig. 2. The original (uncorrected) SHEBA k values as a function of stratification, where $<z>$ is the geometric mean of the five measurement heights and L is the median value of the five Obukhov lengths. The line is (6).

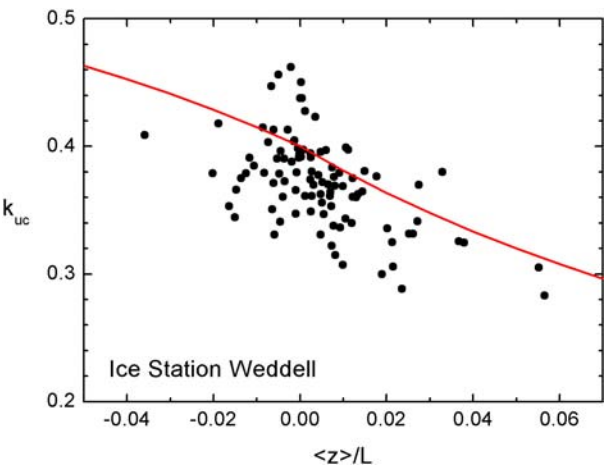

Fig. 3. The original (uncorrected) Ice Station Weddell k values as a function of stratification. As in Fig. 2, $<z>$ is the geometric mean of the profile levels, and the line is (6). The Obukhov length L comes from one eddy-correlation measurement. This plot shows only 100 points because L values were not available for all the ISW points in Fig. 1.

Here, k_{uc} denotes an original, uncorrected k value, and k_{sc} is the stability-corrected value. Figure 4 demonstrates that this manipulation has now removed the stability effects in our measurements of the von Kármán constant.

We can now redo Fig. 1 with these corrected von Kármán constants. Figure 5 shows the results. Our data still seem to change behavior at small values of the roughness Reynolds number and tend to approach the aerodynamically smooth value of 0.421 that McKeon et al. (2004) obtain. At large Re_*, our k values still decrease with Re_* much as the results from Oncley et al. (1996). Frenzen and Vogel's (1995a) data suggest a weaker Re_* dependence.

Since our data seem to be constant for $Re_* < 6.0$ and to decrease for $Re_* \geq 6.0$, we did a least-square fit of k versus Re_* for $Re_* \geq 6.0$. Figure 5 also shows this fitted relation, identified as the "Best Fit."

From (3), (4), (8), and the definition of the roughness Reynolds number, $u_* z_0 / \nu$, we realize that the k values and the Re_* values depicted in Fig. 5 share common variables and may, therefore, have built-in correlation. Using methods that Hicks (1978) and Andreas (2002) describe, we have evaluated the artificial correlation between k and Re_* for the same set that we used for the least-square fit (i.e., for cases with $Re_* \geq 6.0$). Figure 5 also shows the artificial correlation required by these shared variables.

This artificial correlation is statistically indistinguishable from the computed best fit for the $Re_* \geq 6.0$ cases. In other words, we cannot explain the variability in our stability-corrected k values as a dependence on the measured roughness Reynolds number because the correlation we see between these two variables seems totally artificial.

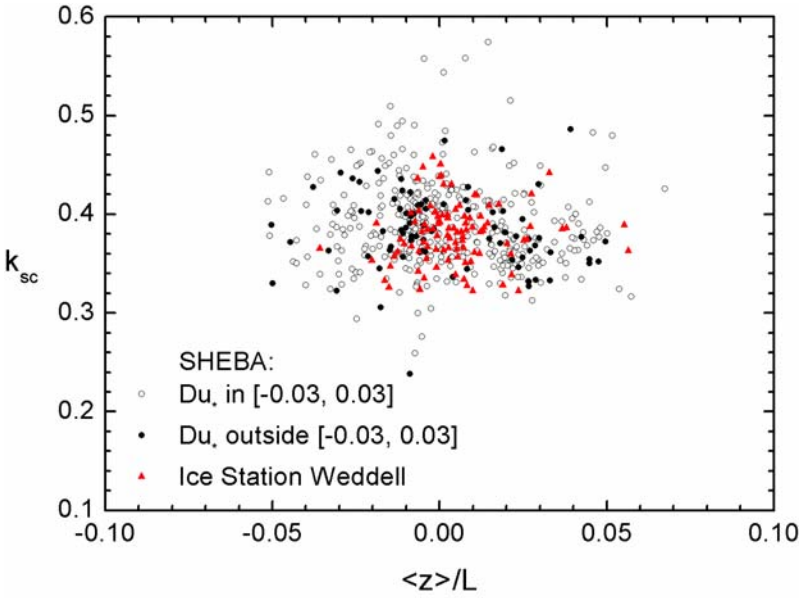

Fig. 4. The von Kármán constants depicted in Figs. 1–3 are here corrected for stratification effects using (7) and (8). The plot contains 453 SHEBA points and 100 ISW points.

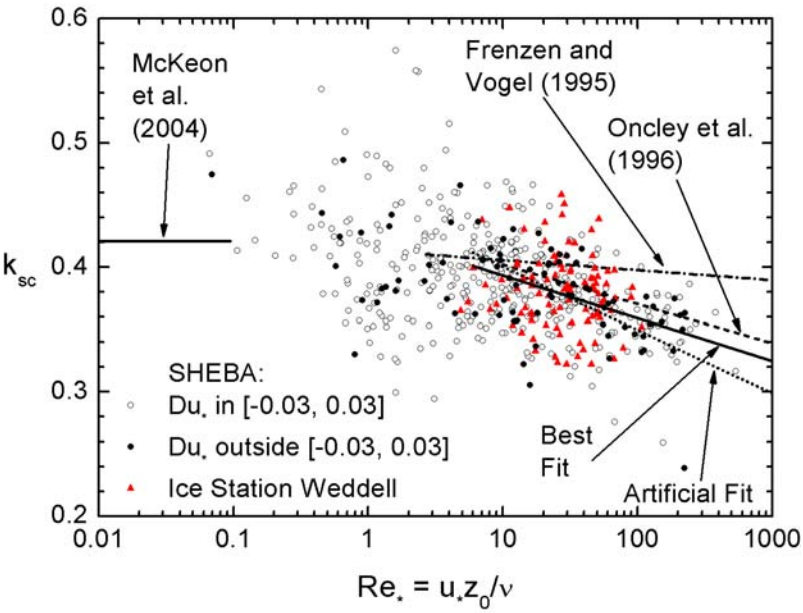

Fig. 5. The stability-corrected SHEBA and Ice Station Weddell values of the von Kármán constant are plotted against measured values of the roughness Reynolds number. The plot also shows tendencies and Reynolds number ranges for the k values that McKeon et al. (2004), Frenzen and Vogel (1995a), and Oncley et al. (1996) deduce. The "Best Fit" line depicts the least-square fit of the data for which $Re_* \geq 6.0$. The "Artificial Fit" line shows the correlation implied if the shared variables used to compute k_{sc} and Re_* are assumed to be independent of each other.

4. BULK ESTIMATES OF Re_*

Because there are theoretical reasons why the von Kármán constant should depend on roughness Reynolds number, we try another way to document this dependence: We evaluate u_* and z_0, and thus Re_*, from a bulk flux algorithm. The bulk flux method (e.g., Fairall et al. 1996) derives from Monin-Obukhov similarity theory. The fluxes of momentum (τ, also called the surface stress) and sensible (H_s) and latent (H_L) heat are expressed as

$$\tau \equiv \rho u_*^2 = \rho C_{Dr} U_r^2 , \qquad (9a)$$

$$H_s = \rho c_p C_{Hr} U_r (\Theta_s - \Theta_r) , \qquad (9b)$$

$$H_L = \rho L_v C_{Er} U_r (Q_s - Q_r) . \qquad (9c)$$

In these, ρ is the air density; c_p, the specific heat of air at constant pressure; L_v, the latent heat of sublimation (over sea ice, remember); U_r, Θ_r, and Q_r, the mean wind speed, potential temperature, and specific humidity at reference height r; and Θ_s and Q_s, the temperature and humidity at the surface. Equation (9a) also shows how we compute the friction velocity with the bulk flux algorithm.

The crux of the bulk flux method is specifying the transfer coefficients for momentum (C_{Dr}, also called the drag coefficient) and for sensible (C_{Hr}) and latent (C_{Er}) heat. We report our full parameterizations for these elsewhere (Andreas et al. 2003, 2004a, 2004b, 2004c). But briefly, for the summer SHEBA data, when the sea ice is free of snow, is melting, and is pocked with leads and melt ponds, we predict C_{Dr} as a function of ice concentration (Andreas et al. 2003). For the Ice Station Weddell and winter SHEBA data, we predict C_{Dr} from

$$C_{Dr} = \frac{k^2}{\left[\ln\left(\frac{r}{z_0}\right) - \psi_m\left(\frac{r}{L}\right)\right]^2} , \qquad (10)$$

where here k = 0.40 and we use the parameterization in Andreas et al. (2004a, 2004c) to predict z_0.

For all the SHEBA and ISW data, we predict the scalar transfer coefficients from

$$C_{Hr} = \frac{k^2}{\left[\ln\left(\frac{r}{z_T}\right) - \psi_h\left(\frac{r}{L}\right)\right]\left[\ln\left(\frac{r}{z_0}\right) - \psi_m\left(\frac{r}{L}\right)\right]} ,(11a)$$

$$C_{Er} = \frac{k^2}{\left[\ln\left(\frac{r}{z_Q}\right) - \psi_h\left(\frac{r}{L}\right)\right]\left[\ln\left(\frac{r}{z_0}\right) - \psi_m\left(\frac{r}{L}\right)\right]} .(11b)$$

To predict the roughness lengths for temperature (z_T) and humidity (z_Q) required in these, we use Andreas's (1987) theoretical model (also Andreas 2002). For the stability functions ψ_m and ψ_h in (10) and (11), we use the same functions that Jordan et al. (1999) and Andreas et al. (2004b) use. For the SHEBA summer cases, we convert our prediction of C_{Dr} to z_0 to implement (11). Also realize that, although we are interested here only in estimating u_* and z_0, we must use all equations (9), (10), and (11) because L depends on u_*, H_s, and H_L and the solution, thus, involves iterative calculations.

Figure 6 shows our stability-corrected k values plotted as a function of the roughness Reynolds numbers resulting from these bulk flux calculations (i.e., $Re_{*,bulk}$). Although the ISW data in this figure show a slight decrease in k_{sc} with $Re_{*,bulk}$, the SHEBA data and the combined ISW-SHEBA set show no correlation between k_{sc} and $Re_{*,bulk}$. Another point is that this bulk flux calculation does not reproduce the very large and very small roughness Reynolds numbers evident in Fig. 5. Finally, in many applications, bulk estimates of the turbulent fluxes, the roughness lengths, and thus Re_* are all we would have available. That is, Fig. 6 represents how any variability in the von Kármán constant would be predicted in practice.

5. CONCLUSIONS

We have estimated the uncertainty in individual measurements of the stability-corrected von Kármán constant and place it at ±18%. That is, any of our individual measurements of k is uncertain by about ±0.07. Ninety-three percent of the k_{sc} values depicted in Fig. 6 are within ±0.07 of 0.39. Therefore, perhaps the scatter in our plots reflects measurement uncertainties rather than the influence of other variables on k. The fact that we cannot establish a dependence on the roughness Reynolds number makes this a palatable alternative conclusion.

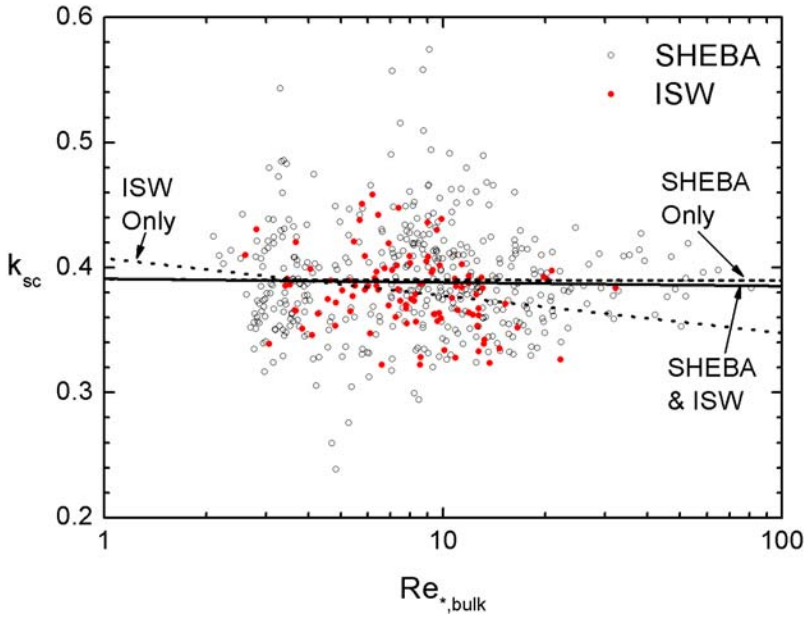

Fig. 6. The stability-corrected von Kármán constants plotted against corresponding bulk estimates of the roughness Reynolds number. The lines show the least-square fits of the Ice Station Weddell data, the SHEBA data, and the combined set.

Table 1. Summary of stability-corrected values of the von Kármán constant. The right-most column gives the approximate 95% confidence interval for the respective average.

		k			
Data Set	Number	Average	Standard Deviation of Population	Standard Deviation of Mean	2×Standard Deviation of Mean
SHEBA:					
All	453	0.389	0.042	0.002	0.004
For Du_* in $[-0.03,0.03]$	83	0.383	0.038	0.004	0.008
Ice Station Weddell	100	0.381	0.030	0.003	0.006
Combined Sets	553	0.387	0.041	0.002	0.004

Nevertheless, we do conclude that the von Kármán constant in the atmospheric surface layer is smaller than the canonical value of 0.40. Table 1 summarizes the data on which we base this result. The entire SHEBA data set, the best SHEBA data (those collected in a constant stress layer), the ISW data, and the entire combined ISW-SHEBA set all agree that the average von Kármán constant is 0.38–0.39 with very small uncertainty in this mean value. We therefore recommend 0.387 ± 0.004 as our best estimate of k. Coincidentally, Frenzen and Vogel (1995b) conclude $k = 0.387 \pm 0.010$ from 29 measurements.

Contrary to the hope we expressed at Wageningen, however, we have been unable to reconcile the significant differences between von Kármán constants measured in the atmosphere and in the lab. As the most recent example, McKeon et al. (2004) report on two high-quality data sets obtained in the Princeton Superpipe in aerodynamically smooth flow—one set was their own, and the other was from Zagarola and Smits (1998). The von Kármán constant they deduce from these laboratory sets, 0.421 ± 0.002, is simply inexplicably incompatible with the lower values found in the last decade in the atmospheric surface layer (Frenzen and Vogel 1995a, 1995b; Oncley et al. 1996), including our own.

6. ACKNOWLEDGMENTS

The U.S. National Science Foundation supported this work with awards to CRREL, NOAA/ETL, and NPS. The U.S. Department of the Army also supported Andreas and Claffey through projects at CRREL.

7. REFERENCES

Andreas, E. L, 1987: A theory for the scalar roughness and the scalar transfer coefficients over snow and sea ice. *Bound.-Layer Meteor.*, **38**, 159–184.

____, 2002: Parameterizing scalar transfer over snow and ice: A review. *J. Hydrometeor.*, **3**, 417–432.

____, and K. J. Claffey, 1995: Air-ice drag coefficients in the western Weddell Sea: 1. Values deduced from profile measurements. *J. Geophys. Res.*, **100**, 4821–4831.

____, C. W. Fairall, P. S. Guest, and P. O. G. Persson, 1999: An overview of the SHEBA atmospheric surface flux program. Preprints, *13th Symp. on Boundary Layers and Turbulence*, Dallas, TX, Amer. Meteor. Soc., 550–555.

____, K. J. Claffey, C. W. Fairall, P. S. Guest, R. E. Jordan, and P. O. G. Persson, 2002: Evidence from the atmospheric surface layer that the von Kármán constant isn't. Preprints, *15th Symp. on Boundary Layers and Turbulence*, Wageningen, The Netherlands, Amer. Meteor. Soc., 418–421.

____, C. W. Fairall, A. A. Grachev, P. S. Guest, T. W. Horst, R. E. Jordan, and P. O. G. Persson, 2003: Turbulent transfer coefficients and roughness lengths over sea ice: The SHEBA results. Preprints, *7th Conf. on Polar Meteorology and Oceanography*, Hyannis, MA, Amer. Meteor. Soc., CD-ROM 3.11, 9 pp.

____, R. E. Jordan, and A. P. Makshtas, 2004a: Parameterizing turbulent exchange over sea ice: The Ice Station Weddell results. *Bound.-Layer Meteor.*, submitted.

____, ____, and ____, 2004b: Simulations of snow, ice, and atmospheric processes on Ice Station Weddell. *J. Hydrometeor.*, to appear.

____, ____, P. S. Guest, P. O. G. Persson, A. A. Grachev, and C. W. Fairall 2004c: Roughness lengths over snow. Preprints, *18th Conf. on Hydrology*, Seattle, WA, Amer. Meteor. Soc., CD-ROM JP4.31, 8 pp.

Dyer, A. J., 1974: A review of flux-profile relationships. *Bound.-Layer Meteor.*, **7**, 363–372.

Fairall, C. W., E. F. Bradley, D. P. Rogers, J. B. Edson, and G. S. Young, 1996: Bulk parameterization of air-sea fluxes for Tropical Ocean-Global Atmosphere Coupled-Ocean Atmosphere Response Experiment. *J. Geophys. Res.*, **101**, 3747–3764.

Frenzen, P., and C. A. Vogel, 1995a: On the magnitude and apparent range of variation of the von Karman constant in the atmospheric surface layer. *Bound.-Layer Meteor.*, **72**, 371–392.

____, and ____, 1995b: A further note "On the magnitude and apparent range of variation of the von Karman constant." *Bound.-Layer Meteor.*, **73**, 315–317.

Hicks, B. B., 1978: Some limitations of dimensional analysis and power laws. *Bound.-Layer Meteor.*, **14**, 567–569.

Jordan, R. E., E. L Andreas, and A. P. Makshtas, 1999: Heat budget of snow-covered sea ice at North Pole 4. *J. Geophys. Res.*, **104**, 7785–7806.

McKeon, B. J., J. Li, W. Jiang, J. F. Morrison, and A. J. Smits, 2004: Further observations on the mean velocity distribution in fully-developed pipe flow. *J. Fluid Mech.*, **501**, 135–147.

Oncley, S. P., C. A. Friehe, J. C. Larue, J. A. Businger, E. C. Itsweire, and S. S. Chang, 1996: Surface-layer fluxes, profiles, and turbulence measurements over uniform terrain under near-neutral conditions. *J. Atmos. Sci.*, **53**, 1029–1044.

Panofsky, H. A., 1963: Determination of stress from wind and temperature measurements. *Quart. J. Roy. Meteor. Soc.*, **89**, 85–94.

Paulson, C. A., 1970: The mathematical representation of wind speed and temperature profiles in the unstable atmospheric surface layer. *J. Appl. Meteor.*, **9**, 857–861.

Persson, P. O. G., C. W. Fairall, E. L Andreas, P. S. Guest, and D. K. Perovich, 2002: Measurements near the Atmospheric Surface Flux Group tower at SHEBA: Near-surface conditions and surface energy budget. *J. Geophys. Res.*, **107** (C10), SHE 21-1–SHE 21-35, doi: 10.1029/2000JC000705.

Tennekes, H., 1973: The logarithmic wind profile. *J. Atmos. Sci.*, **30**, 234–238.

Uttal, T., and 27 others, 2002: Surface Heat Budget of the Arctic Ocean. *Bull. Amer. Meteor. Soc.*, **83**, 255–275.

Zagarola, M. V., and A. J. Smits, 1998: Mean-flow scaling of turbulent pipe flow. *J. Fluid Mech.*, **373**, 33–79.